Open access • Posted Content • DOI:10.1101/2020.09.18.303966

Measuring competitive exclusion in non-small cell lung cancer — Source link

Nathan Farrokhian, Jeff Maltas, Mina N. Dinh, Arda Durmaz ...+8 more authors

Institutions: Case Western Reserve University, Cleveland Clinic, University of Pennsylvania, University of Oxford

Published on: 29 Sep 2021 - bioRxiv (Cold Spring Harbor Laboratory)

Topics: Population

Dose dependent evolutionary game dynamics modulate competitive release in cancer therapy

Nathan Farrokhian[1], Jeff Maltas[2], Patrick Ellsworth[1], Arda Durmaz[1], Mina Dinh[2], Masahiro Hitomi[2], Artem Kaznatcheev[2,3,*], Andriy Marusyk[4,*], and Jacob G Scott[1,2,5,*]

[1]Case Western Reserve School of Medicine, Cleveland, OH, USA
[2]Department of Translational Hematology and Oncology Research, Cleveland Clinic, Cleveland, OH, USA
[3]Department of Computer Science, University of Oxford, Oxford, UK
[4]Department of Cancer Physiology, Moffitt Cancer Center, Tampa, FL, USA
[5]Department of Radiation Oncology, Cleveland Clinic, Cleveland, OH, USA
[*]scottj10@ccf.org, andriy.marusyk@moffitt.org,

ABSTRACT

Therapeutic strategies for tumor control have traditionally assumed that maximizing reduction in tumor volume correlates with clinical efficacy. Unfortunately, this rapid decrease in tumor burden is almost invariably followed by the emergence of therapeutic resistance. Evolutionary based treatment strategies work to delay this inevitability by promoting the maintenance of tumoral heterogeneity. While these strategies have shown promise in recent clinical trials, they often rely on biological conjecture and intuition to derive parameters. Reproducibility of the success seen with this treatment paradigm is contingent on formal elucidation of underlying subclonal interactions. One such consequence of these interactions, "competitive release", is an evolutionary phenomenon that describes the unopposed proliferation of resistant populations following maximally tolerated systemic therapies. While often assumed in evolutionary models of cancer, here we show the first empiric evidence of "competitive release" occurring in an *in vitro* tumor environment. We found that this phenomenon is modulated by both drug dose and initial population composition. As such, we observed that monotypic fitness differentials were insufficient to accurately predict the outcomes of this phenomenon. Instead, derivation of underlying frequency dependent evolutionary game dynamics is essential to understand resulting sub-population shifts through time. To evaluate the impact of these non-autonomous growth behaviors over longer time series, we used a range of commonly employed growth models, some of which are the foundation of ongoing clinical trials. While useful for identifying persistent qualitative features, we observed significant fragility and model specific behaviors that limited the ability of these models to make consistent quantitative predictions, even when the parameters were empirically derived.

Introduction

Given our current understanding of intratumoral heterogeneity, treatment resistance after continuous dose chemotherapy is an expected consequence. Genomic instability[1], inherent to the development of most cancer[2–5], results in the accumulation of a wide range of aberrations within a single tumor population.[6] While only a small subset of these randomly distributed changes will contribute directly to driving carcinogenesis, this diverse population comprised of phenotypically distinct subclones results in increased resilience of the overall tumor population across a wide range of external stressors.[7–9]

These distinct subclones do not live, grow, or reproduce in isolation. With this diverse cellular population comes a diverse range of intercellular interactions. Complex systems can often not be fully described empirically, and their dynamics are usually impossible to intuit from descriptions of their parts. In these situations, mathematical models have historically played a role. Specifically, solutions to evolutionary games have proven to be an effective method for elucidating the evolutionary consequences of interactions in large multicellular ecosystems, such as fisheries[10] and game reserves.[11] More recently, these evolutionary game theoretical models have begun being utilized to gain insight into phenotypic shifts that occur within tumor ecosystems.[12–15] Within this framework, it is understood that particular properties selected for within a population are not only directed by environmental conditions, but also evolve in manner dependent on the frequency of other subtypes present within the population.[16] This frequency dependent growth acts to shape treatment-naïve tumor ecosystems and influences inevitable development of resistance in post-treatment environments.[17–20] Furthermore, as traditional treatment protocols continue to fail, more evolutionary-based treatments that rely on judicious treatment schedules and cooperative dynamics between populations have gained in popularity[21–26]. One such hypothesized idea is competitive release.[27] Originally coined as “character release”,[28] competitive release occurs when two or more populations are originally competing for the same resources, however as the stress of competition is diminished (such as via the extinction of a population through treatment) one population is able to

expand and become more dominant. It is thought that selective killing of sensitive cells during therapy removes competitive restrictions on resistant populations, allowing for their outgrowth and subsequent therapeutic failure. While intuitive in theory and observed in bacteria[29], empiric evidence of the dynamics that underlie this phenomenon in cancer have, to our knowledge, yet to be elucidated.

Dynamic therapeutic protocols using models of this type have already made their way into the clinic with promising results.[25] While this highlights the value of game theoretical models for treatment optimization, the specific model was selected and parameterized mainly based on biological conjecture and intuition. Instead, we hypothesize that for each clinical condition, a different model and parameters would be needed to accurately capture intratumoral dynamics. As such, reproducibility of this initial success across different tissues and environmental contexts is contingent on our ability to elucidate subclonal interactions in the lab prior to transitioning to clinical practice. These quantitatively and qualitatively distinct interactions greatly influence the evolutionary trajectory of the tumor and subsequent growth patterns; therefore, incorrect characterization can unintentionally lead to worsened treatment outcomes.

Recently, we developed an *in vitro* evolutionary game assay that admits direct measure of the underlying ecological dynamics within heterogeneous tumor environments.[26] Here we utilize these techniques with a model non-small cell lung cancer (NSCLC) population to better understand phenotypic equilibria in treatment naïve populations and subsequent emergence of resistance, which has proven to be virtually inevitable in clinic.[30–32] Specifically, we sought to elucidate "competitive release" as it relates to competing subclones within a tumor. While foundational to many evolutionary based therapeutic strategies, this phenomenon had yet to be empirically observed or quantitatively derived. Further, we sought to characterize the diverse range of ecological interactions that occur across various microenvironmental contexts to increase accuracy of therapeutic predictions and avoid pitfalls that would result in therapeutic failure.

Box 1: Experimentally Derived Evolutionary Game Dynamics

Tracking individual subclones in heterotypic cultures:
To track differential growth dynamics of two populations in the same culture, each population was transduced with a vector encoding a different heritable fluorescent protein. For this experiment, the resistant and parental cells were made to stably express mCherry and EGFP respectively. The expression of these proteins was linked to nuclear localization signal (NLS) repeats for localization of the fluorescent signal into each cell's nuclei. This increases resolution and accuracy of cell number counts at higher confluency. Once plated together in heterotypic culture, each subclone could be tracked through time in their respective fluorescent channel using time-lapse microscopy systems [Figure 1.1].

Translating image information into growth rates:
Cell number counts were extracted from each fluorescent image at each time point throughout the time series. Exponential growth rates where determined via semi-log regression of change in cell number against change in time (hours) using the Theil-sen estimator [Figure 1.2].

Fitness functions - growth as a function of population composition:
To find the dependence of fitness on the frequency of subclonal interaction, least squares regressions were performed on the growth rate against the initial proportion of parental in each well [Figure 1.3]. This regression was weighted against the inverse of the errors ($\frac{1}{\sigma^2}$) associated with each growth rate. The resulting linear equations describe growth as a function of the initial proportion of the opposing subclone:

$$\hat{w}_P = A + k(1-p) \tag{1}$$
$$\hat{w}_R = D + kp \tag{2}$$

These linear equations can be rearranged into fitness functions, which describe the fitness ($\hat{w}$) of a sub clone as a function of the initial proportion (p) of interacting cells within the population.

$$\hat{w_P} = Ap + B(1-p) \tag{3}$$
$$\hat{w_R} = Cp + D(1-p) \tag{4}$$

Game theoretical payoff matrix:
To clearly represent the fitness outcome of specific interactions, payoff matrices corresponding to each of the different conditions can be derived from the resulting fitness functions. For example, the fitness outcome of parental cells interacting with one another occurs when $p = 1$, which translates to $\hat{w_P} = A$. Similarly, the fitness outcome of when parental interacts with resistant occurs when $p = 0$, which translates to $\hat{w_P} = B$.

$$\begin{array}{cc} & \begin{array}{cc} \text{P} & \text{R} \end{array} \\ \begin{array}{c} \text{P} \\ \text{R} \end{array} & \begin{pmatrix} A & B \\ C & D \end{pmatrix} \end{array} \tag{5}$$

The errors associated with the on-diagonal payoffs are equivalent to the uncertainty of the intercept values, σ_A and σ_D for parental and resistant respectively. The errors associated with the off-diagonal payoffs were derived by propagating the uncertainty of both the intercept and slope through the addition:

$$\sigma_B = \sigma_A + \sigma_k \tag{6}$$
$$\sigma_C = \sigma_D + \sigma_k \tag{7}$$

Results/Discussion

Ecological interactions define phenotypic equilibrium in treatment naive tumor populations

The lung adenocarcinoma cell line PC9 was selected to represent NSCLC driven by activating mutations in the EGFR gene. To recapitulate underlying clonal diversity, parental and resistant lineages were derived from an identical starting population. The resistant lineage was cultured in the presence of 1μM gefitinib for a minimum of 6 months. The parental lineage was grown in parallel in a matched volume of DMSO. A high initial dose was chosen to select for preexisting resistant populations rather than drug tolerant cells.[33]

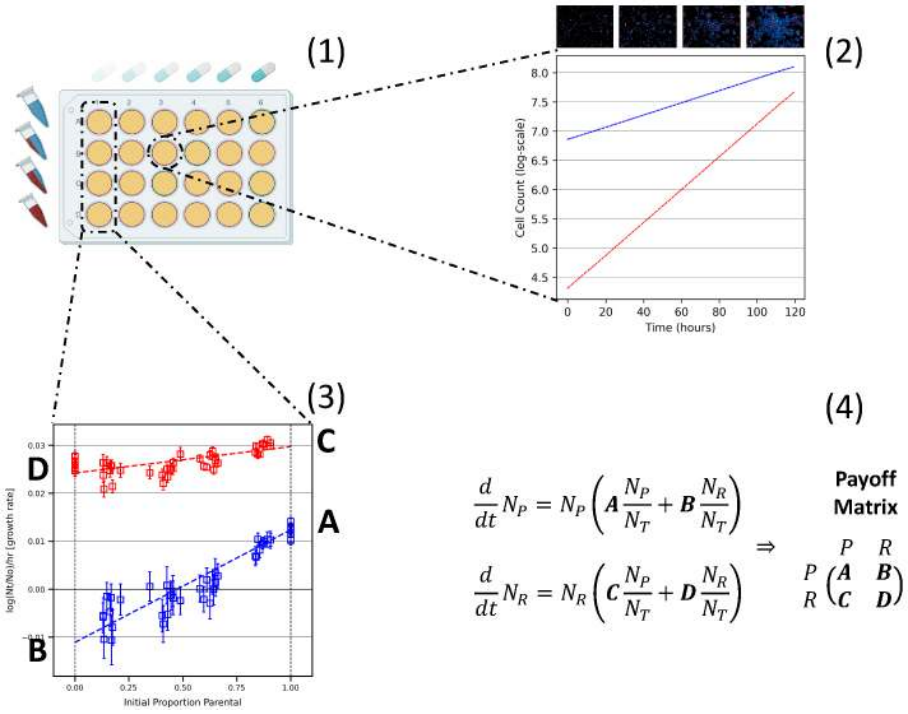

Figure 1. **Experimentally derived subclonal interactions: an evolutionary game assay**. **(1)** Co-cultures of both subclones were plated across full spectrum of initial proportions and in a range of different different drugs/concentrations. **(2)** Time-lapse microscopy was utilized to capture population composition at different time points. Cell number counts were extracted from each fluorescent image and plotted against elapsed time to derive subclonal growth rates in each well. **(3)** Growth rates of all wells in a given condition were plotted against initial proportion parental. **(4)** Fitness functions and associated payoff matrices from derived via least squared regression and intercepts of $p = 0$ and $p = 1$.

Evaluation of monotypic cultures revealed significantly slower growth of the resistant subclone compared to parental in the absence of drug [Figure 2A]. This finding provides evidence for a fitness cost associated with the resistant phenotype in this model population of NSCLC, which is an oft made assumption in models of resistance development. While these reduced growth kinetics had been previously suggested in treatment resistant populations of EGFR driven NSCLC,[34] this feature may not be generalizable across all NSCLC types.[26] Given this differential fitness and expected similar resource needs, traditional Darwinian evolution would predict extinction of the less fit subclone if cell autonomous growth was assumed. Interestingly, our observations in heterotypic cultures revealed that interactions with parental in this environment positively impacted resistant fitness ($D < C$ in game matrix [eq. 5]) in a frequency dependent manner [Figure 2B] allowing for a heterotypic equilibrium which would not be predicted from evaluation of monotypic growth alone.

One of the most important features of this eco-evolutionary dynamic is that the fitness of the resistant population becomes statistically indistinguishable from the parental as the population approaches $p = 1$. As a consequence, entries A, B, and C in the resulting game matrix [eq. 5] are not significantly different from one another. In other words, retention of the resistant phenotype in the population is promoted by parental cells, but only low proportions of the resistant phenotype can be maintained. This finding supports the notion of stable heterogeneous treatment-naïve tumor populations that allow for pre-existence of growth suppressed resistant subclones.

Chemotherapeutic resistance as a consequence of competitive release

Given this quantitative evidence to support a heterogeneous, treatment-naïve tumor population comprised of both subclones at equilibrium, we sought to model the emergence of resistance after exposure to treatment. Our derived resistant subclone was evolved under the selective pressure of continuous 1μM gefitinib therapy and, as expected, monotypic cultures at this dose clearly show a significant fitness advantage of the resistant cells [Figure 3A].

Heterotypic cultures show positive growth rates of both subclones while the population harbors majority parental [Figure 3A]. At these proportions, the fitness of the resistant subclone is still significantly greater than that of the parental population. Over time, this differential fitness results in greater representation of the resistant subclone in the population [Figure 3A]. Once the proportion crosses a critical threshold, which can be quantified from the derived game matrix, the fitness of the parental

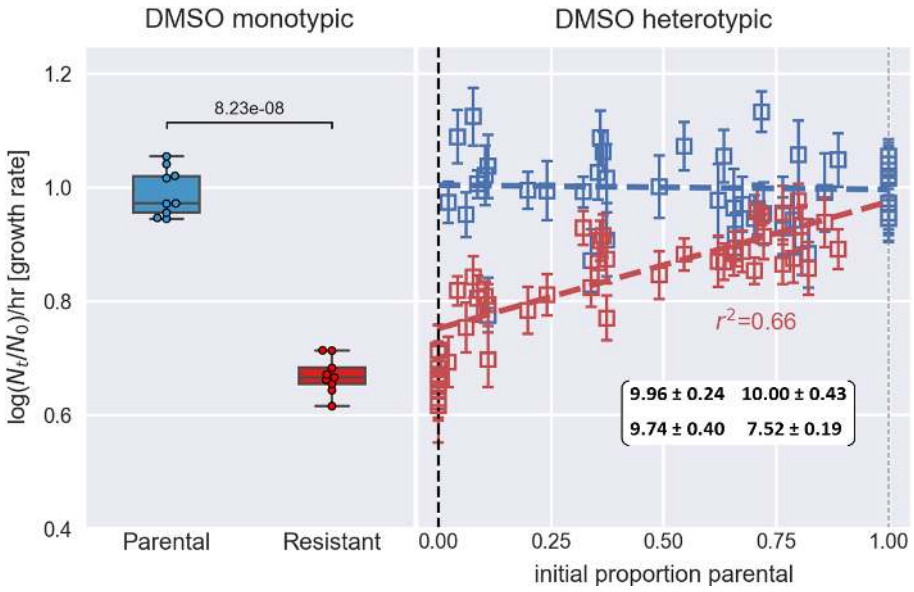

Figure 2. **Ecological interactions significantly alter resistant clone growth dynamics, which promotes coexistence of both subtypes in treatment-naïve environments.** Monoculture cultures in DMSO shows significant difference in growth between subclones ($p < 0.05$), highlighting the cost associated with the resistant phenotype. Heterotypic cultures in DMSO reveal strong frequency dependent interactions where the resistant subclone benefits greatly from interaction with parental cells, promoting retention of the resistant phenotype at low proportions within the population. Plotted values were normalized against mean monotypic parental growth in DMSO. Values in displayed game matrix have been scaled $\times 10$ for ease of comparison.

lineage becomes negative, resulting in its rapid extinction [Figure 3B].

As such, the eco-evolutionary dynamics that prevented the resistant population from increasing in representation can be altered with exposure to gefitinib. This introduced environmental stressor releases resistant cells from the competitive interactions that prevented their expansion in treatment-naïve conditions, allowing for increased representation. We believe this to be the first empiric demonstration of this phenomenon in cancer, though it is one that is often referred to in the theoretical literature, and has been observed recently in a simple bacterial population.[29]

Exploiting eco-evolutionary dynamics to modulate competitive release

Continual administration of chemotherapeutic agents at their maximum tolerated dose (MTD) has become the mainstay in many therapy regimens. While these strategies may find success in the short-term, they often have no significant impact in the long term due to the inevitability of treatment resistance.[35] We investigated why this may be the case through heterotypic dose escalation experiments.

In monotypic cultures, increasing the dose of gefitinib had no significant impact on resistant growth rate [Figure 4A], but did significantly impact the growth of parental, albeit with diminishing returns. While doses above 0.25μM had minimal additional effect on cell autonomous parental growth, these higher doses greatly enhanced interactions between the subclones, which manifests as an increase in the absolute value of the fitness functions' slopes [eq. 4]. This results in negative parental growth occurring at higher parental proportions, greatly increasing the rate of competitive release. Interestingly, although the monotypic resistant growth rates were not significantly different at any of the doses, they derived increasing benefit from interacting with the parental population in heterotypic cultures. A similar phenomenon has been observed in bacterial populations, in that high densities of sensitive bacterial cells boost the probability of existing resistant cell outgrowth under selective pressures.[36]

While these findings provide evidence for the inevitability of resistant outgrowth for all doses of gefitinib tested, increasing the dose greatly impacted the speed at which the parental population was extinguished from the population. This potential to modulate time to parental extinction and subsequent competitive release has significant implications for the long-term success of therapeutic strategies.

To explore the outcomes of these specific features further, time expansion of the derived fitness functions was done with both replicator dynamics [eq. 9] and a practical derivative of the Lotka-Volterra (LV) equation [eq. 11] that allows for competitive exclusion of interacting species. Both of these models attempt to predict population level trends through time, the former with the assumption of infinite expansion and the latter constraining the populations to a strict maximum. *In vivo* tumor growth likely falls somewhere in between, as nutrient availability and space constrains growth in a more fluid manner through mechanisms

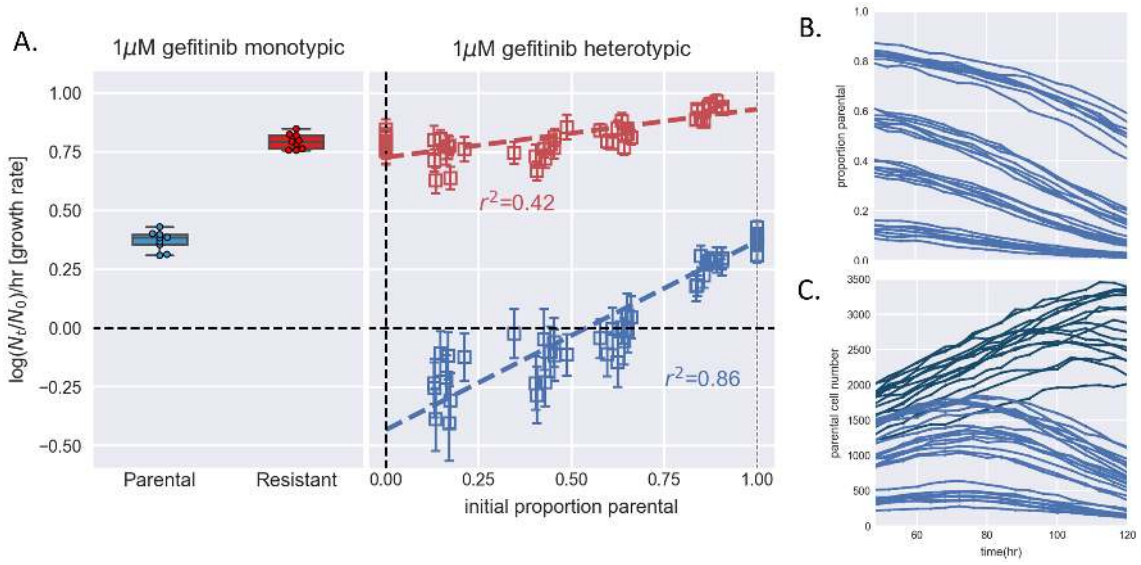

Figure 3. **Frequency dependent interactions in gefitinib drive extinction of the parental lineage and subsequent competitive release of resistant cells A.** Monotypic cultures in 1μM gefitinib show significant reduction in parental growth compared to resistant. Heterotypic cultures reveal resistant cells greatly driving down parental growth in a frequency dependent manner. Plotted values were normalized against mean monotypic parental growth in DMSO. **B.** Proportional shifts through time reveal competitive release of resistant subclone and inevitable extinction of parental from the population. **C.** Rate of parental extinction increases significantly at specific proportional thresholds, as predicted by the value at which the fitness function crosses $y = 0$.

such as angiogenesis. Given the inability of either of these models to perfectly recapitulate realistic growth conditions, they are inadequate to confidently make specific numerical predictions of *in vivo* outcomes. Instead, their value lies in the ability to identify qualitative dynamics that persist across this spectrum of growth behaviors.

For each model, relative time to extinction was determined for the range of doses, where extinction is defined as proportion of the population, p, dropping below < 0.01. This definition of extinction was adopted to evaluate this model because within this framework, true parental extinction does not occur if the corresponding fitness function never reaches a negative value between $0 \leq p \leq 1$. As expected, the replicator equation predicted faster extinction of the sensitive population at higher doses [Figure 5A]. The LV model told a similar story while providing hypothetical information regarding total tumor burden given assumptions about carrying capacities, which are very difficult to estimate and have large effects on quantitative aspects [Figure 5B]. When the carrying capacities of both subclones are equal ($K_p = K_r = K_{max}$), time to extinction occurs at identical time scales compared to the replicator equations [Figure 5C]. To evaluate the impact of frequency dependent growth, the results were contrasted against models run with monotypic growth parameters [Figure 5C]

Unfortunately, this assumption of equal carrying capacity is likely untrue of *in vivo* contexts, as the carrying capacity for each cell type would likely change as a function of environmental stressors. To capture this, we varied the relative carrying capacity of the two populations to be a ratio of the cell autonomous rates scaled by their maximum rate in the absence of drug [Figure 5D]. With these parameters, there is a significant decrease in the absolute tumor burden across all doses, a response that is more characteristic of what would be expected in the clinical setting. The time to parental extinction still followed the same trend as before, albeit at different time scales [Suppl. Fig. 10]. This sensitivity to even small alterations in the the relative carrying capacities underscores the fragility of this model when attempting to make specific quantitative predictions. Interestingly, there is less of an absolute decrease in the tumor burden after initiation of lower dose therapy; however, this decrease is sustained for a longer period of time compared to higher doses [Figure 5E]. This is largely dictated by the slower extinction of the parental population, whose presence continues to limit outgrowth of the resistant population - a feature that persisted across all models tested.

Insight into pair-wise interactions can inform therapeutic protocols

Given the shifts in strength of eco-evolutionary interactions that were observed as a function of changing gefitinib dose, we sought out to measure the frequency-dependent interactions of these two populations in a diverse array of drugs. We explored second-line therapies because of potential therapy implications of collateral sensitivities, a focus of our group.[37–40]

For example, monotypic cultures of parental and gefitinib resistant cell lines in 0.6μM etoposide and 0.2μM pemetrexed show fairly similar sensitivity profiles; however, their heterotypic growth tell a significantly different story [Figure 6]. In

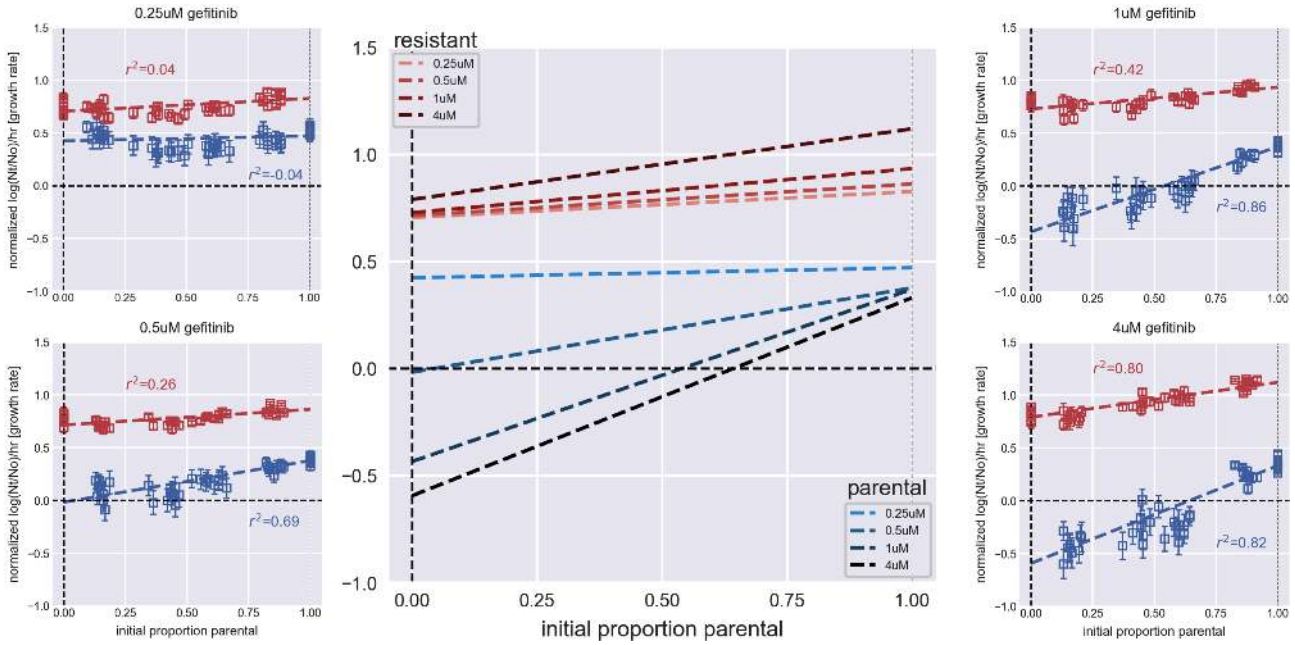

Figure 4. **Dose dependent alteration of ecological dynamics in gefitinib modulate competitive release in this model system of EGFR driven NSCLC.** This extinction is specifically driven by frequency dependent interactions. **Outer plots:** Non-cell autonomous growth patterns of parental and resistant cells in 0.25μM, 0.5μM, 1μM, and 4μ of gefitinib. Plotted values were normalized against mean monotypic parental growth in DMSO. **Center plot:** Comparison of resulting fitness functions across the range of doses highlights how intratumoral interactions between subclones can be altered through dose escalation of selective pressure. The effect of increased dose was far more pronounced in heterotypic cultures as compared to monotypic cultures.

pemetrexed, parental growth has an inverse relationship with the proportion resistant in the population. As $p \to 0$, the parental and resistant fitness become statistically indistinguishable. As such, it is likely that a fixed point exists within this region where both parental and resistant populations have equal fitness. Competitive release of the parental population with extinction of resistant will only occur if the parental proportion surpasses this fixed point. Conversely, 0.6μM etoposide will result in increased representation of the parental across all frequencies.

In practice, these eco-evolutionary dynamics have the potential to drive radically different outcomes. Based on monotypic fitness measurements, both of these drugs appear to be equally good candidates for sensitization phases of dosing protocols. While competitive release is possible in pemetrexed, the timing of the sensitization will be critical in determining its success. If significant expansion of the resistant population is allowed during the treatment phase, then sensitization will fail as the fitness of parental becomes statistically indistinguishable from that of resistant as $p \to 0$.

When devising adaptive therapeutic regimens, it is important to not only identify the quality of interactions in the different drugs, but also develop understanding of how the drug concentration can modulate these interactions. Etoposide highlights important shifts that can occur at different drug doses [Figure 7]. At low doses of etoposide, the interactions follow a qualitative dynamic known in the game theory literature as "Harmony II" resulting in inevitable extinction of the resistant subclone. As the dose is increased, the game switches to one known as "Leader I", which contains an evolutionary stable strategy (ESS). The resulting net fitness in this condition maintains heterogeneity at a wide range of proportions. If the dose is increased further, there is disruption of this equilibrium with competitive release of the resistant cell population as the parental cells are driven to extinction. These three distinct qualitative outcomes at different doses of the same drug demonstrates how dynamic the underlying interactions can be and, in turn, highlighting the value of pre-clinical elucidation.

Discussion

Similar to how Lotka and Volterra both independently observed the dependence of prey on predator,[41] so to has the importance of interactions within the diverse tumor ecosystem become apparent to the field of cancer biology.[42,43] The outcome of these interactions shape this ecosystem, creating continuous feedback that defines the overall composition and growth characteristics.[44] As a result of this continuous feedback, increased resolution on the ecological underpinnings of the tumor environment is accompanied with the ability to manipulate and drive this dynamic system to clinically desirable endpoints.[45]

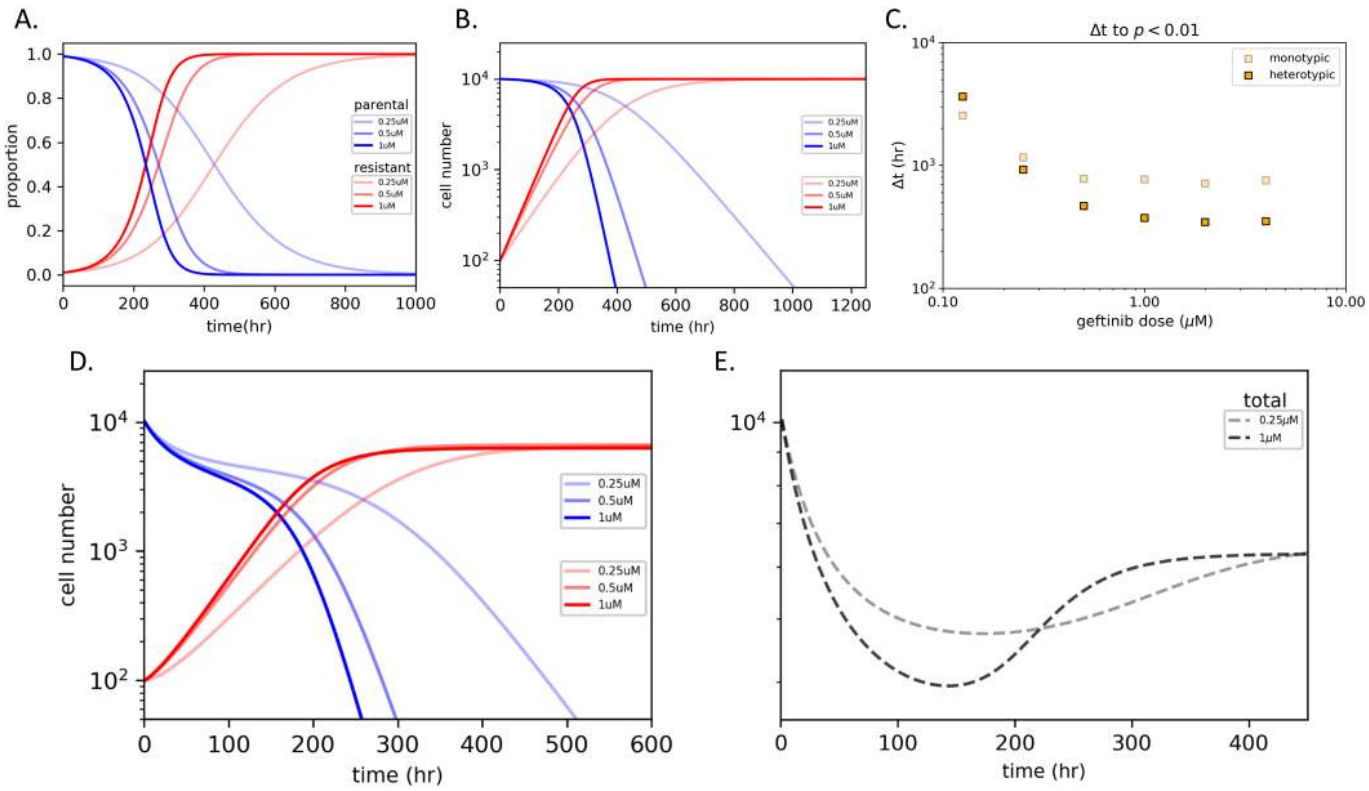

Figure 5. **Evaluation of growth models with empirically derived parameters highlights rapid acceleration of competitive release via non-cell autonomous interactions and demonstrates persistence of qualitative features across the spectrum of models tested.** The same initial parameters were used for each model ($p = 0.99$). **A.** Replicator dynamics showing proportional shifts of both competing cell populations over time in three gefitinib doses. **B.** Lotka-Volterra (LV) model of outgrowth in constrained environments with equal carrying capacities ($K_p = K_r$). **C.** Time to extinction (defined as the proportion of the population, p, dropping below 0.01) across a range of gefitinib doses was determined and compared between cell autonomous (monotypic) and non-autonomous (heteorotypic) growth. **D.** LV model with unequal carrying capacities ($K_i = K_{max}\alpha_i$ where $\alpha_i = r_{mono}/r_{max}$). **E.** Estimates for changes in total tumor burden for relative LV model in 0.25μM and 1μM of gefitinib. Treatment with the lower dose of 0.25μM had a smaller initial response to therapy, but longer overall response due to delayed parental extinction and maintenance of heterogeneity over a longer period of time.

We found that gefitinib resistance is associated with a significant, quantifiable cost in drug-free monotypic cultures. One might posit that competition with the more fit sensitive subclone in treatment-naïve environments would promote extinction and allow for only transient existence. Instead, we observed that the parental cells positively impacted the growth of the resistant lineage in a frequency dependent manner, which provides evidence that these non-cell autonomous behaviors promote phenotypic equilibria that result in the maintenance of underlying tumor heterogeneity. Without these non-cell autonomous growth dynamics, costly resistance conferring mutations that arise stochastically would quickly disappear from the population. We show that a small proportion of resistant cells are able to coexist; however, their reliance on the parental population prevents increasing representation: competition prevents their outgrowth.

In keeping with traditional game theoretical literature, this interaction can conceptually be thought of as a public goods game in which the parental population is producing a "good" that the resistant lineage can free-ride, providing them with a significant increase in fitness.[46] In a sense, the incurred resistant phenotype cost is "reimbursed" through interaction with the parental population.

While the exact mechanism of this hypothesized "public good" is unknown, the resulting effect on the fitness of the resistant lineage is significant – allowing for their preservation at low frequency in treatment-naïve populations, while simultaneously preventing their outgrowth. Mechanisms for public goods have been theorized to include growth factor production[47]

Altering tumoral heterogeneity can change the quality of these interactions and allow for outgrowth of this previously suppressed population. Resistance to targeted therapy is thought to arise from this described outgrowth due to the selective killing of sensitive tumor cells. Specifically, we observed that introduction of gefitinib into heterotypic cultures resulted in frequency dependent killing of the sensitive cell, which allowed for unopposed proliferation of resistant subclone through a phenomenon known in the literature as competitive release.[27] While remaining agnostic to the specific resistance mechanisms,

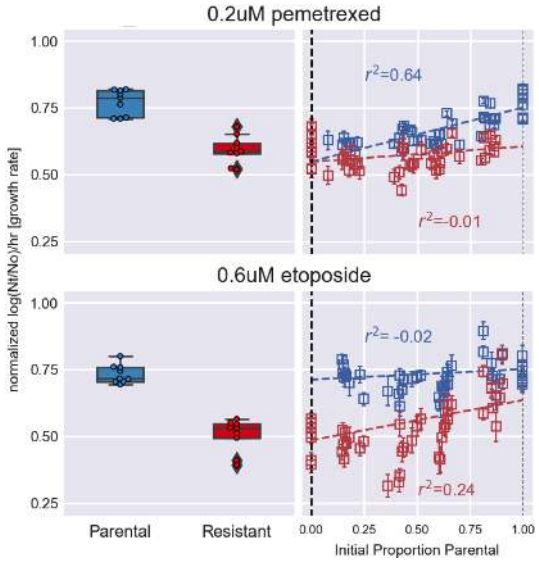

Figure 6. While seemingly similar monotypic profiles, frequency dependent growth reveals significantly different underlying eco-evolutionary dynamics.

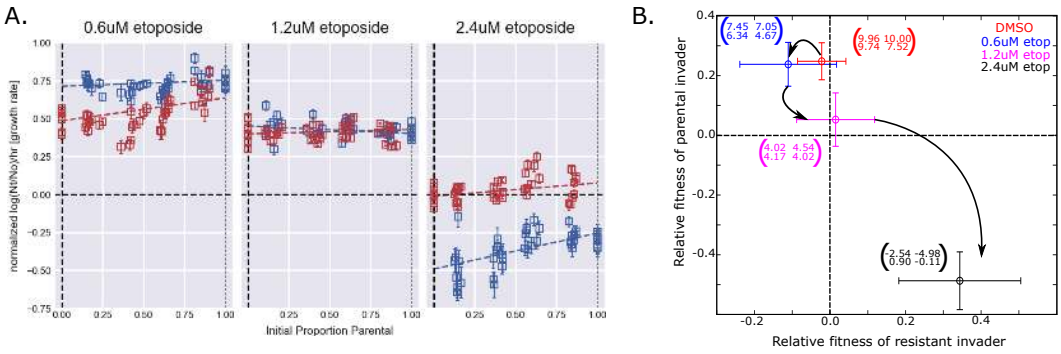

Figure 7. A. Here we show escalating dosage of etoposide result in qualitatively different growth dynamics. At low doses the ancestor out-competes the resistant strain no matter the parental proportion. However, as dose increases the resistant strain becomes dominant, out-competing the ancestor at all proportions. B. We visualize this dose-dependent behavior in the game space. The x-axis is the relative fitness of a resistant invader (quantified as C-A in the game matrix). The y-axis is the relative fitness of a parental invader (quantified as B-D in the game matrix).

this uninhibited proliferation offers an explanation for the eventual failure to targeted therapies seen across most cancer types.[48–50]

Interestingly, we found that altering the intensity of the selection pressure through dose modulation can promote and maintain heterogeneity without compromising response to therapy - a finding that has been observed in clinic[51] and studied in pre-clinical models[24], but is incompletely understood. At lower concentrations of gefitinib, the fitness of the parental was not dramatically impacted by the presence of resistant cells. With dose escalation, the strength of interaction between the two types increased in a dose dependent manner resulting in faster rates of parental extinction from the tumor population. Theoretical growth models with these experimentally derived parameters predicted a blunted initial response to therapy at lower doses; however, longer retention of the parental subclone prolonged total therapy response by delaying outgrowth of the resistant population and subsequent competitive release. This feature of delayed resistant outgrowth was not sensitive to model selection and persisted under assumptions of either infinite or restricted populations.

The implications of this specific feature are especially important in the development of dynamic protocols.[52] For example, bio-markers utilized for tracking resistance may only surpass detectable thresholds once a significant resistant population has been established. We observed that the higher the dose, the more likely the parental population will have been driven to extinction by the time these thresholds are reached, guaranteeing failure of subsequent sensitization phases. As such, *designing specific interventions without quantitative derivation of underlying interactions can result in worsened therapeutic outcomes,*

even if the qualitative assumptions are correct. Only through elucidation of these dynamics can we proceed to the development of protocols that have the power to promote and sustain heterogeneity, rather than eliminate it.

Further, our observations show that monotypic fitness differentials are insufficient to predict ecological shifts in specific environments. Assumption of cell autonomous growth can result in non-optimal scheduling, or in some cases, completely unexpected clinical outcomes. Many of the interactions observed within this model system of EGFR driven NSCLC greatly deviate from what biological intuition may predict. As such, elucidation of underlying effective ecological interactions[53,54] is critical to admit clinical decision making and avoid pitfalls that result in therapeutic failure.

While often discussed in theory and assumed based on intuition, this is the first empiric evidence of competitive release occurring in an empirical cancer system to our knowledge. Further, we observed that this phenomenon can be modulated in a dose dependent manner to alter time to extinction in a way that was incompletely predicted from monotypic growth differentials, as underlying intratumoral interactions can prevent or enhance this ecological outcome [Figure 8]. As such, it can be concluded that intuition is not sufficient to apply these concepts clinically. Instead, ecological parameters should be determined empirically to ensure accurate characterization of population shifts through time.

By working with, rather than against, the underlying eco-evolutionary dynamics, we can move towards therapeutic protocols that favor tumor control by maintaining treatable populations.[55] Translation of these quantitative models to the *in vivo* setting can provide the necessary framework to make shifts towards these treatment paradigms possible.[56]

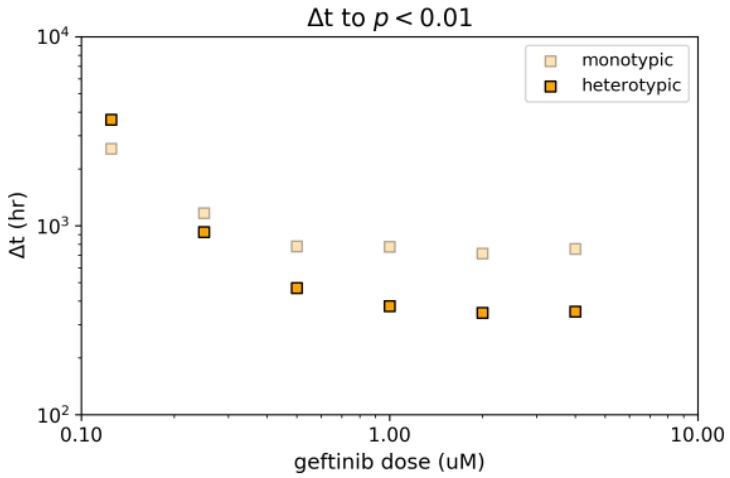

Figure 8. **Dose dependent modulation of competitive release is incompletely predicted from monotypic growth rates.**

Methods

Cell lines: All cells were cultured in Roswell Park Memorial Institute (RPMI) media supplemented with 10% fetal bovine serum (FBS) and 1% penicillin/streptomycin.

Parental and resistant cell lines were established from the same initial population of PC9 cells (Sigma-Aldrich 90071810). Resistant population was cultured in 1uM of gefitinib (Cayman 13166) for greater than 6 months, until a population of stably growing cells was observed. Resulting subpopulations exhibited noticeable visual morphological differences in culture. The parental population was cultured in parallel in matched volumes of dimethyl sulfoxide (DMSO) (Sigma-Aldrich 276855) for the same duration as a vehicle control.

Resulting resistant and parental subclones underwent lentiviral transduction with plasmid vectors encoding EGFP- and mCherry- fluorescent proteins with attached nuclear localization sequence (plasmids were a gift from Andriy Marusyk's lab at Moffitt Cancer Center). Derivative cell lines with heritable fluorescent protein expression were selected for in puromycin (MP Biomedical 100552).

Experimental design: Cells were harvested at 70-80% confluence, stained with trypan blue (Corning 25-900-CI), and manually counted with a hemocytometer (Bright-Line Z359629). Mono- and co-cultures of each subclone were seeded across a range of initial relative proportions in 96-well formats and allowed to attach for 18-24 hours.

Wells were treated with the following drugs: gefitinib, paclitaxel (Cayman 10461), etoposide (Cayman 12092), pemetrexed (Cayman 26677), and lapatinib (Cayman 11493) as single agents. Plates were loaded into a BioSpa 8 Automated Incubator

(BioTek Instruments). Time-lapse microscopy images were obtained for bright field, GFP, and mCherry via Cytation 5 Imaging Reader (BioTek) every 4 hours over the course of 5 days.

Image Processing: Images were processed with Gen5 (BioTek) and the open-source software ImageJ.[57] Image sets were duplicated, background subtracted, contrasted limited adaptive histogram equalization (CLAHE), and thresholded. Despeckle filter was applied to the now binary images, watershed segmentation was performed, and raw cell numbers were extracted from the resulting image sets.

Evolutionary Game Assay: To quantify the dynamics in our *in vitro* environments, we utilized the experimental game assay developed by Kaznatcheev et al..[26] Initial proportions were calculated for each well individually from the first image. Time series of raw cell numbers were normalized against initial number in each well. Linear regression was performed using the Theil-sen estimator on the semi-log cell change against time. The slope of the resulting linear function (with its corresponding 95% confidence interval) was translated as the growth rate across the time series, which were normalized against the average of six parental monoculture wells that were run on each plate.

To find the dependence of fitness on the frequency of subclonal interaction, least squares regressions were performed on the growth rate against the initial proportion of parental in each well. This regression was weighted against the inverse of the errors ($\frac{1}{\sigma^2}$) associated with each growth rate. The resulting linear equations describe fitness as a function of the initial proportion of the opposing subclone:

$$\hat{w}_P = A + kr$$
$$\hat{w}_R = D + kp$$

The intercepts of these functions translate to monoculture fitness, which are the symmetric payoffs within a game matrix. The asymmetric payoffs can be translated as the fitness values when r and p are equal to 1:

$$B = A + k$$
$$C = D + k$$

These linear equations can be rearranged to describe the fitness ($\hat{w}$) of a sub clone as a function of the initial proportion (p) of interacting cells within the population.

$$\hat{w_P} = Ap + B(1-p)$$
$$\hat{w_R} = Cp + D(1-p)$$

Payoff matrices corresponding to each of the different conditions can be derived by setting p equal to one and zero for both equations. For example, the symmetric payoff for parental occurs when $p = 1$, which translates to $\hat{w_P} = A$.

$$\begin{array}{cc} & \begin{array}{cc} \text{P} & \text{R} \end{array} \\ \begin{array}{c} \text{P} \\ \text{R} \end{array} & \begin{pmatrix} A & B \\ C & D \end{pmatrix} \end{array}$$

The errors associated with the on-diagonal payoffs are equivalent to the uncertainty of the intercept values, σ_A and σ_D for parental and resistant respectively. The errors associated with the off-diagonal payoffs were derived by propagating the uncertainty of both the intercept and slope through the above addition [eq.8].

Growth models: To synthesize hypothetical tumor growth using our measured frequency dependent growth rates, we used two distinct models, one that allowed for infinite growth and one that limited total volume to a strict maximum. This was done to identify salient qualitative features that persisted across this spectrum of models, rather than make specific quantitative predictions.

For infinite growth, replicator dynamics were chosen:

$$\dot{p} = p(\hat{w_P} - \langle w \rangle) \tag{8}$$
$$\dot{r} = (1-p)(\hat{w_R} - \langle w \rangle) \tag{9}$$

where $\langle w \rangle$ denotes average population fitness such that:

$$\langle w \rangle = p\hat{w_P} + (1-p)\hat{w_R}$$

For growth that is strictly limited to a maximum, a Lotka-Volterra derivative[58] was utilized that included frequency dependent growth:

$$\frac{dN_p}{dt} = N_p * r_p \left[1 - \frac{N_p}{K_p} - \frac{N_r r_r}{K_p r_p}\right] \tag{10}$$

$$\frac{dN_r}{dt} = N_r * r_r \left[1 - \frac{N_r}{K_r} - \frac{N_p r_p}{K_r r_r}\right] \tag{11}$$

where r_p and r_r are non-cell autonomous growth rates determined by values of the game matrix such that:

$$r_p = A\left(\frac{N_p}{N_p + N_r}\right) + B\left(\frac{N_r}{N_p + N_r}\right)$$

$$r_r = C\left(\frac{N_p}{N_p + N_r}\right) + D\left(\frac{N_r}{N_p + N_r}\right)$$

While this model is insensitive specific carrying capacity values, it is highly sensitive to the relative value of the carrying capacity. Given that both subclones occupy similar space in an *in vitro* environment, we first evaluated the condition where the carrying capacities were equal to one another:

$$K_p = K_r$$

The above assumption likely does not translate to *in vivo* conditions. Instead, the carrying capacities of each type would likely vary across different environments. To capture this phenomenon, the carrying capacity was scaled for each condition:

$$K_i = K_{max}\alpha_i$$

where K_{max} is the maximum carrying capacity across all conditions and α_i is a weighting term that scales this maximum using a ratio of current monoculture growth rate against the maximum growth rate:

$$\alpha_i = \frac{r_{mono}}{r_{max}}.$$

References

1. Cahill, D. P., Kinzler, K. W., Vogelstein, B. & Lengauer, C. Genetic instability and darwinian selection in tumours. *Trends cell biology* **9**, M57–M60 (1999).
2. Loeb, L. A. Mutator phenotype may be required for multistage carcinogenesis. *Cancer research* **51**, 3075–3079 (1991).
3. Marusyk, A., Almendro, V. & Polyak, K. Intra-tumour heterogeneity: a looking glass for cancer? *Nat. Rev. Cancer* **12**, 323–334 (2012).
4. Almendro, V., Marusyk, A. & Polyak, K. Cellular heterogeneity and molecular evolution in cancer. *Annu. Rev. Pathol. Mech. Dis.* **8**, 277–302 (2013).
5. Loeb, L. A. Human cancers express a mutator phenotype: hypothesis, origin, and consequences. *Cancer research* **76**, 2057–2059 (2016).
6. McGranahan, N. & Swanton, C. Biological and therapeutic impact of intratumor heterogeneity in cancer evolution. *Cancer cell* **27**, 15–26 (2015).
7. Marusyk, A. & Polyak, K. Tumor heterogeneity: causes and consequences. *Biochimica et Biophys. Acta (BBA)-Reviews on Cancer* **1805**, 105–117 (2010).
8. Gerlinger, M. *et al.* Intratumor heterogeneity and branched evolution revealed by multiregion sequencing. *N Engl j Med* **366**, 883–892 (2012).
9. Burrell, R. A., McGranahan, N., Bartek, J. & Swanton, C. The causes and consequences of genetic heterogeneity in cancer evolution. *Nature* **501**, 338–345 (2013).

10. Lotka, A. J. Analytical note on certain rhythmic relations in organic systems. *Proc. Natl. Acad. Sci.* **6**, 410–415 (1920).

11. Lima, S. L. Putting predators back into behavioral predator–prey interactions. *Trends Ecol. & Evol.* **17**, 70–75 (2002).

12. Basanta, D. *et al.* Investigating prostate cancer tumour–stroma interactions: clinical and biological insights from an evolutionary game. *Br. journal cancer* **106**, 174–181 (2012).

13. Kaznatcheev, A., Scott, J. G. & Basanta, D. Edge effects in game-theoretic dynamics of spatially structured tumours. *J. The Royal Soc. Interface* **12**, 20150154 (2015).

14. Kaznatcheev, A., Vander Velde, R., Scott, J. G. & Basanta, D. Cancer treatment scheduling and dynamic heterogeneity in social dilemmas of tumour acidity and vasculature. *Br. journal cancer* **116**, 785–792 (2017).

15. Pacheco, J. M., Santos, F. C. & Dingli, D. The ecology of cancer from an evolutionary game theory perspective. *Interface focus* **4**, 20140019 (2014).

16. Bohl, K. *et al.* Evolutionary game theory: molecules as players. *Mol. BioSystems* **10**, 3066–3074 (2014).

17. Basanta, D., Gatenby, R. A. & Anderson, A. R. Exploiting evolution to treat drug resistance: combination therapy and the double bind. *Mol. pharmaceutics* **9**, 914–921 (2012).

18. Basanta, D. & Anderson, A. R. Exploiting ecological principles to better understand cancer progression and treatment. *Interface focus* **3**, 20130020 (2013).

19. Marusyk, A. *et al.* Non-cell-autonomous driving of tumour growth supports sub-clonal heterogeneity. *Nature* **514**, 54–58 (2014).

20. Janiszewska, M. *et al.* Subclonal cooperation drives metastasis by modulating local and systemic immune microenvironments. *Nat. cell biology* **21**, 879–888 (2019).

21. Martin, R. B. Optimal control drug scheduling of cancer chemotherapy. *Automatica* **28**, 1113–1123 (1992).

22. Yurtsev, E. A., Chao, H. X., Datta, M. S., Artemova, T. & Gore, J. Bacterial cheating drives the population dynamics of cooperative antibiotic resistance plasmids. *Mol. systems biology* **9**, 683 (2013).

23. Maltas, J. & Wood, K. B. Pervasive and diverse collateral sensitivity profiles inform optimal strategies to limit antibiotic resistance. *PLOS Biol.* **17**, 1–34, DOI: 10.1371/journal.pbio.3000515 (2019).

24. Enriquez-Navas, P. M. *et al.* Exploiting evolutionary principles to prolong tumor control in preclinical models of breast cancer. *Sci. translational medicine* **8**, 327ra24–327ra24 (2016).

25. Zhang, J., Cunningham, J. J., Brown, J. S. & Gatenby, R. A. Integrating evolutionary dynamics into treatment of metastatic castrate-resistant prostate cancer. *Nat. communications* **8**, 1–9 (2017).

26. Kaznatcheev, A., Peacock, J., Basanta, D., Marusyk, A. & Scott, J. G. Fibroblasts and alectinib switch the evolutionary games played by non-small cell lung cancer. *Nat. ecology & evolution* **3**, 450–456 (2019).

27. West, J., Ma, Y. & Newton, P. K. Capitalizing on competition: An evolutionary model of competitive release in metastatic castration resistant prostate cancer treatment. *J. Theor. Biol.* **455**, 249–260 (2018).

28. Grant, P. R. Convergent and divergent character displacement. *Biol. journal Linnean Soc.* **4**, 39–68 (1972).

29. Hansen, E., Karslake, J., Woods, R. J., Read, A. F. & Wood, K. B. Antibiotics can be used to contain drug-resistant bacteria by maintaining sufficiently large sensitive populations. *PLOS Biol.* **18**, 1–20, DOI: 10.1371/journal.pbio.3000713 (2020).

30. Morgillo, F., Della Corte, C. M., Fasano, M. & Ciardiello, F. Mechanisms of resistance to egfr-targeted drugs: lung cancer. *ESMO open* **1** (2016).

31. Wu, S.-G. & Shih, J.-Y. Management of acquired resistance to egfr tki–targeted therapy in advanced non-small cell lung cancer. *Mol. cancer* **17**, 38 (2018).

32. Santoni-Rugiu, E. *et al.* Intrinsic resistance to egfr-tyrosine kinase inhibitors in egfr-mutant non-small cell lung cancer: differences and similarities with acquired resistance. *Cancers* **11**, 923 (2019).

33. Hata, A. N. *et al.* Tumor cells can follow distinct evolutionary paths to become resistant to epidermal growth factor receptor inhibition. *Nat. medicine* **22**, 262 (2016).

34. Chmielecki, J. *et al.* Optimization of dosing for egfr-mutant non–small cell lung cancer with evolutionary cancer modeling. *Sci. translational medicine* **3**, 90ra59–90ra59 (2011).

35. Bozic, I. & Nowak, M. A. Resisting resistance. *Annu. Rev. Cancer Biol.* **1**, 203–221 (2017).

36. Alexander, H. K. & Maclean, R. C. Stochastic bacterial population dynamics restrict the establishment of antibiotic resistance from single cells. *Proc. Natl. Acad. Sci.* (2020).

37. Nichol, D. *et al.* Antibiotic collateral sensitivity is contingent on the repeatability of evolution. *Nat. communications* **10**, 1–10 (2019).

38. Scarborough, J. A. *et al.* Identifying states of collateral sensitivity during the evolution of therapeutic resistance in ewings sarcoma. *bioRxiv* (2020).

39. Yoon, N., Krishnan, N. & Scott, J. Modeling collaterally sensitive drug cycles: shaping heterogeneity to allow adaptive therapy. *bioRxiv* (2020).

40. Dhawan, A. *et al.* Collateral sensitivity networks reveal evolutionary instability and novel treatment strategies in alk mutated non-small cell lung cancer. *Sci. reports* **7**, 1–9 (2017).

41. Kingsland, S. Alfred j. lotka and the origins of theoretical population ecology. *Proc. Natl. Acad. Sci.* **112**, 9493–9495 (2015).

42. Gatenby, R. A. & Maini, P. K. Mathematical oncology: cancer summed up. *Nature* **421**, 321–321 (2003).

43. West, J. *et al.* Towards multidrug adaptive therapy. *Cancer research* **80**, 1578–1589 (2020).

44. Scott, J. & Marusyk, A. Somatic clonal evolution: A selection-centric perspective. *Biochimica et Biophys. Acta (BBA)-Reviews on Cancer* **1867**, 139–150 (2017).

45. Korolev, K. S., Xavier, J. B. & Gore, J. Turning ecology and evolution against cancer. *Nat. Rev. Cancer* **14**, 371–380 (2014).

46. Gerlee, P. & Altrock, P. M. Extinction rates in tumour public goods games. *J. The Royal Soc. Interface* **14**, 20170342 (2017).

47. Archetti, M., Ferraro, D. A. & Christofori, G. Heterogeneity for igf-ii production maintained by public goods dynamics in neuroendocrine pancreatic cancer. *Proc. Natl. Acad. Sci.* **112**, 1833–1838 (2015).

48. Vasan, N., Baselga, J. & Hyman, D. M. A view on drug resistance in cancer. *Nature* **575**, 299–309 (2019).

49. Cree, I. A. & Charlton, P. Molecular chess? hallmarks of anti-cancer drug resistance. *BMC cancer* **17**, 1–8 (2017).

50. Gatenby, R. & Brown, J. The evolution and ecology of resistance in cancer therapy. *Cold Spring Harb. perspectives medicine* **8**, a033415 (2018).

51. Kerbel, R., Klement, G., Pritchard, K. & Kamen, B. Continuous low-dose anti-angiogenic/metronomic chemotherapy: from the research laboratory into the oncologyclinic. *Annals Oncol.* **13**, 12–15 (2002).

52. Gluzman, M., Scott, J. G. & Vladimirsky, A. Optimizing adaptive cancer therapy: dynamic programming and evolutionary game theory. *Proc. Royal Soc. B* **287**, 20192454 (2020).

53. Kaznatcheev, A. Two conceptions of evolutionary games: reductive vs effective. *bioRxiv* 231993 (2017).

54. Kaznatcheev, A. Effective games and the confusion over spatial structure. *Proc. Natl. Acad. Sci.* **115**, E1709–E1709 (2018).

55. Staňková, K., Brown, J. S., Dalton, W. S. & Gatenby, R. A. Optimizing cancer treatment using game theory: A review. *JAMA oncology* **5**, 96–103 (2019).

56. Bozic, I. & Wu, C. J. Delineating the evolutionary dynamics of cancer from theory to reality. *Nat. Cancer* **1**, 580–588 (2020).

57. Schindelin, J. *et al.* Fiji: an open-source platform for biological-image analysis. *Nat. methods* **9**, 676–682 (2012).

58. Li, X.-Y. *et al.* Which games are growing bacterial populations playing? *J. The Royal Soc. Interface* **12**, 20150121 (2015).

Supplemental Figures

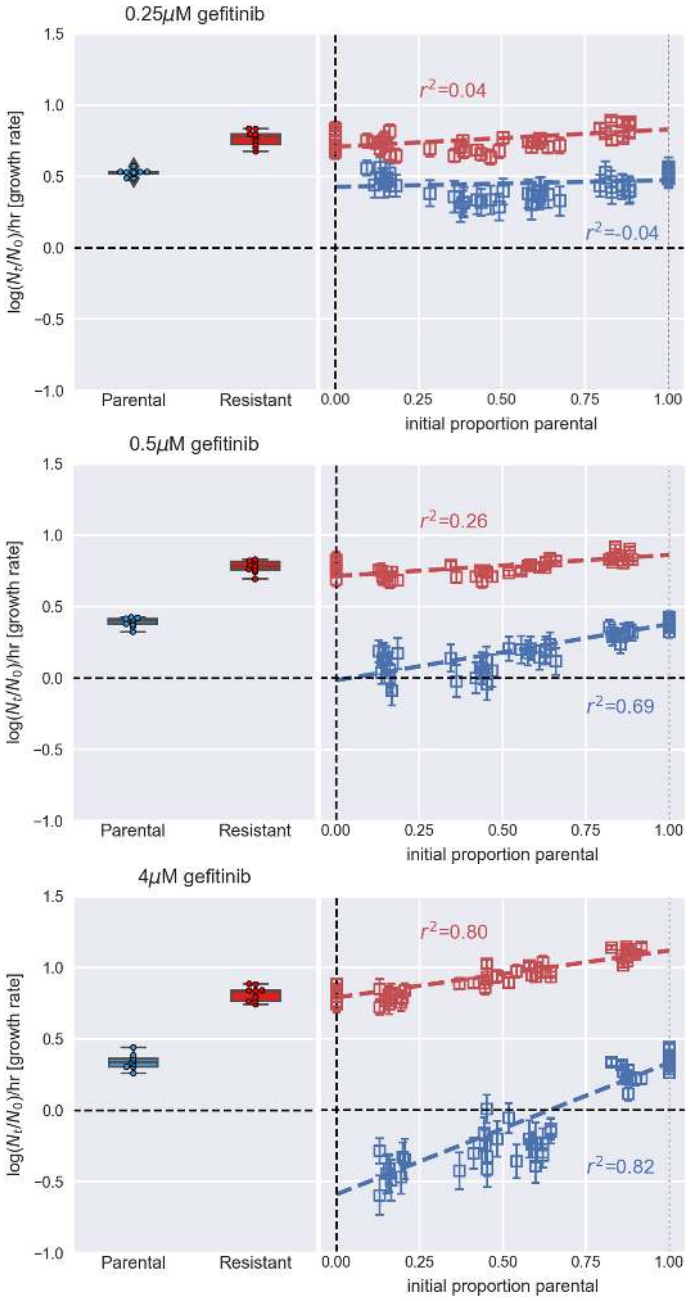

Figure 9. Monotypic and heterotypic fitness differences in gefitinib for 0.25μM, 0.5μM, and 4μM.

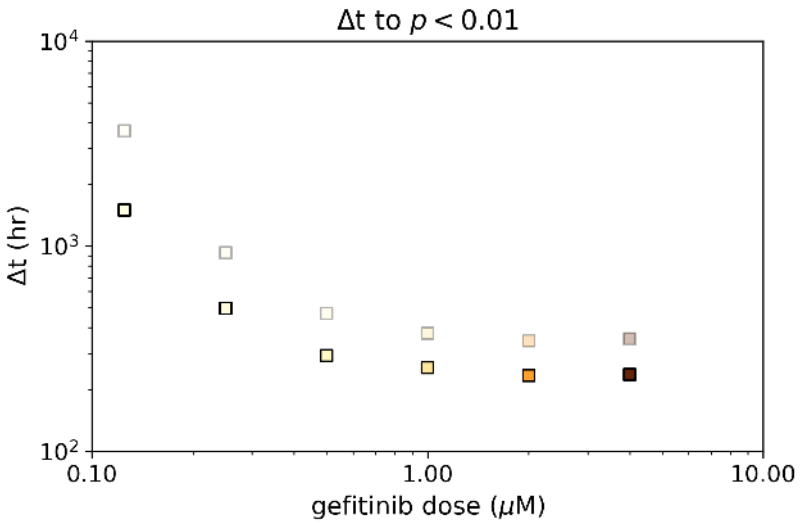

Figure 10. Time to parental extinction with unequal carrying capacities (solid) follows the same qualitative pattern as both replicator and equal carrying capacity models (faded), albeit at different time scales.